TÜBİTAK

Turkish Journal of Chemistry

http://journals.tubitak.gov.tr/chem/

Research Article

Turk J Chem
(2017) 41: 89 – 98

doi:10.3906/kim-1603-127

Highly selective Schiff base derivatives for colorimetric detection of Al^{3+}

Ziya AYDIN[1,*], **Mustafa KELEŞ**[2]
[1]Pazar Vocational School, Recep Tayyip Erdoğan University, Rize, Turkey
[2]Department of Chemistry, Faculty of Arts and Sciences, Osmaniye Korkut Ata University, Osmaniye, Turkey

Received: 28.03.2016 • **Accepted/Published Online:** 15.07.2016 • **Final Version:** 22.02.2017

Abstract: Schiff base derivatives NBAR and NSAR were developed for selective detection of Al^{3+} in aqueous solution. UV-vis spectroscopic studies revealed that NBAR and NSAR showed marked sensitivity and selectivity to Al^{3+} in acetonitrile (ACN)/water (v/v, 1:1, pH 6.80). The NBAR and NSAR receptors bound Al^{3+} in a 2:1 stoichiometry with apparent binding constants 4.09×10^{11} M^{-2} and 1.65×10^{12} M^{-2}, respectively. They also displayed distinct changes in color upon the alteration of free Al^{3+} levels in solution with reversible responses and showed little interference with other metal ions.

Key words: Colorimetric sensor, Schiff base, aluminum, selectivity

1. Introduction

As the most abundant metal in the Earth's crust,[1] aluminum is widely used in water treatment, food additives, deodorants, bleached flour, clinical drugs, and storage/cooking utensils.[2–5] However, free Al^{3+}, which is formed from leaching due to acid rain, is not only detrimental to growing plants[6,7] but also damages the human nervous system and immune system,[8] which can cause many health problems such as Alzheimer disease, Parkinson disease, breast cancer, and dialysis encephalopathy.[9–13] According to the World Health Organization (WHO), the average daily human intake of aluminum is approximately 3–10 mg.[14,15] For these reasons, it is important to develop methods for aluminum detection.

There are several analytical methods for detecting Al^{3+} such as atomic absorbance/emission spectroscopy,[16] inductively coupled plasma-mass spectroscopy (ICP-MS),[17] voltammetry,[18] electron paramagnetic resonance (EPR),[19] and high performance liquid chromatography.[20] Most of these methods require complicated sample-pretreatment procedures, sophisticated synthetic procedures, and high operation costs. In contrast, colorimetric and fluorimetric methods require easier procedures. Organic molecules can be used as sensors (either colorimetric or optical) for the detection of Al^{3+}. For example, fluorescent sensors for Al^{3+} have been reported including rhodamine derivatives,[21–24] quinoline derivatives,[25,26] and coumarins.[27,28] Some organic molecules can also be used as colorimetric chemosensors for Al^{3+};[29,30] however, published reports are rare.

In this paper, we introduce simple and reliable colorimetric chemosensors (NBAR and NSAR) for the detection of Al^{3+} in aqueous media. Schiff base derivatives from cinnamaldehyde have gained attention recently.[31] We linked 4-(dimethylamino)benzaldehyde and 4-(dimethylamino) cinnamaldehyde with 2-amino-5-

*Correspondence: ziya.aydin@erdogan.edu.tr

methylphenol to synthesize the receptors. Both receptors have one nitrogen and one oxygen coordination atoms, which provide binding parts with hard bases for hard acid Al^{3+}. Thus the receptors exhibited good selectivity and sensitivity for Al^{3+}.

2. Results and discussion

2.1. Design and synthesis

The initial goal of the synthesis of NBAR and NSAR was to coordinate to Al^{3+} ions with high binding constants and the receptors were designed based on the principles of coordination chemistry. The receptors have the same binding parts. The only difference is that NBAR has one double bond less than NSAR, indicating that NBAR will show absorption maximum at lower wavelength. The designs of the NBAR and NSAR receptors were carefully developed with a coordination site of one nitrogen and one oxygen atom to afford two five-membered rings in 2:1 binding between the receptors and Al^{3+}. The receptors were synthesized in a one-step procedure with overall yields of 86% and 80% for NBAR and NSAR, respectively (Scheme 1). The structures of the receptors were confirmed by ^{1}H NMR and ^{13}C NMR and mass spectrometry.

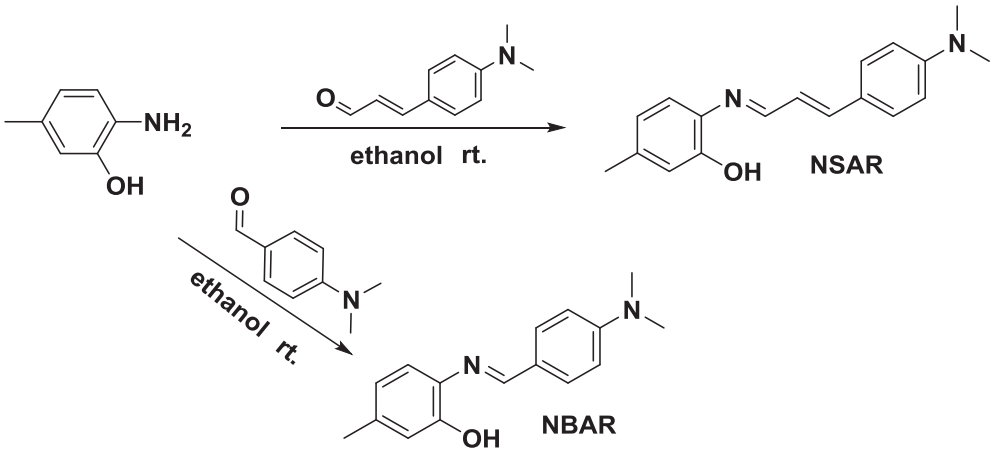

Scheme 1. Synthesis of NBAR and NSAR.

2.2. Spectroscopic and selectivity studies

First, we measured the changes in the absorbance properties of NBAR and NSAR as a result of the addition of various metal ions. The absorption spectra were recorded at ca. 5 min after the addition of 1 equivalent of each of these metal ions. NBAR (20 μM) in ACN/H_2O (v/v, 1:1, pH 6.80) was colorless and exhibited absorption maxima at 356 and 234 nm that may be attributed to $\pi-\pi^*$ charge transfer transition. The metal ions such as Ni^{2+}, Cu^{2+}, Mn^{2+}, Hg^{2+}, Na^{+}, Ca^{2+}, Zn^{2+}, Ag^{+}, Mg^{2+}, Pb^{2+}, K^{+}, Fe^{3+}, Co^{2+}, and Cr^{3+} gave little response to NBAR (Figure 1a). In contrast, with increasing Al^{3+} concentration, the absorbance at 356 nm (ε = 1.20 $\times$ 10^5 M^{-1} cm^{-1}, only NBAR) decreased, while the absorbance at 421 nm (ε = 1.52 $\times$ 10^5 M^{-1} cm^{-1}, NBAR and Al^{3+} 1:1 ratio) increased concomitantly (Figure 1b). This pronounced bathochromic shift of the maximum absorption wavelength could be ascribed to the coordination of Al^{3+}. Meanwhile, an isosbestic point was clearly observed around 391 nm, indicating conversion of the free sensor into the Al(III)-complex is a clean reaction. In addition, this red shift of 65 nm in the absorption behavior changed the color of the resultant solution from colorless to yellow, allowing naked-eye detection of Al^{3+} (Figure 1c).

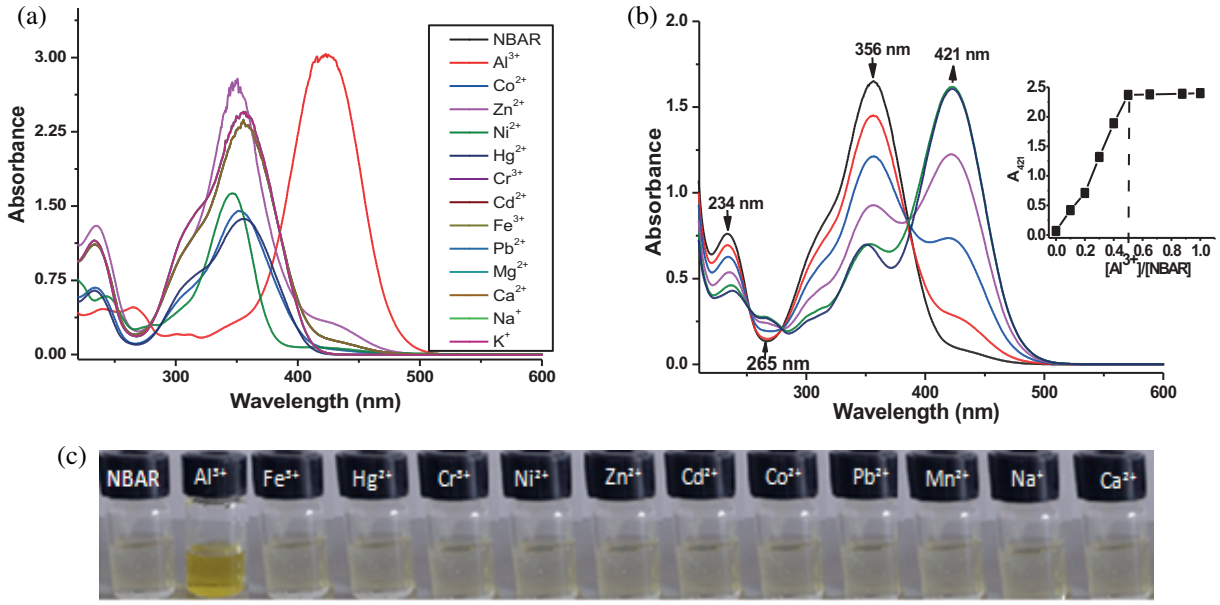

Figure 1. (a) Absorption responses of 20 μM NBAR to various metal ions (20 μM for Zn^{2+}, Cr^{3+}, Ni^{2+}, Hg^{2+}, Fe^{3+}, Al^{3+}, Pb^{2+}, Cd^{2+}, and Co^{2+}; 100 μM for Na^{+}, K^{+}, Mg^{2+}, and Ca^{2+}) in ACN/H_2O (1:1 v/v). (b) UV-vis spectra of NBAR (20 μM) with the addition of various concentrations of $AlCl_3$ (0, 2.5, 5.0, 7.5, 10.0, 12.5, 15.0, 17.5, and 20.0 μM, consecutively) in ACN/H_2O (1:1 v/v). (c) Color changes of 20 μM NBAR with various metal ions.

The effect of pH on NBAR and NBAR-Al^{3+} was investigated at pH range over 1 to 10. The pH of solution was adjusted by adding HCl and NaOH to a mixture solvent of ACN/H_2O (1:1) and was measured by a pH meter. As seen in Figure 2a, the NBAR sensor had no response to hydrogen ions at pH between 5 and 9 but did give a response to hydrogen ions at pH below 4.5. These results demonstrate that Al^{3+} recognition by sensor NBAR is barely interfered with by pH in the range from 4.5 to 9. We also examined the interferences from the other metal ions with NBAR in its response to Al^{3+}. Each of the 13 metal ions was pre-incubated with NBAR before 1 equiv. of Al^{3+} was added; the absorption response was then measured. As shown in Figure 2b, the absorption spectrum of NBAR with Al^{3+} was not affected significantly in the presence of any of the other metal ions tested, demonstrating little interferences from the other metal ions. Obviously, remarkable selectivity for absorption detection of Al^{3+} can be available even in the presence of co-existing metal ions.

We also did the same selective experiments for the sensor NSAR. The changes in the absorption spectra of NSAR with the addition of different metal ions (1 equiv.) in ACN/water (v/v, 1:1, pH 6.80) are shown in Figure 3a. The free NSAR exhibited absorption maxima at 385 and 244 nm; as expected, its absorbance maxima were at a longer wavelength (385 nm) than that of NBAR (356 nm) due to one extra double bond. After adding Al^{3+} to the solution of NSAR, the absorbance at 385 nm ($\varepsilon = 1.78 \times 10^4$ M^{-1} cm^{-1}, only NSAR) decreased, while the absorbance at 502 nm ($\varepsilon = 4.6 \times 10^4$ M^{-1} cm^{-1}, NSAR and Al^{3+} 1:1 ratio) increased concomitantly (Figure 3b). The sensor also gave a response to Hg^{2+}. However, the absorption intensity was a little weaker for Hg^{2+} ($\varepsilon = 1.70 \times 10^4$ cm^{-1} M^{-1}) compared to that for Al^{3+}. In addition, this red shift of 117 nm in the absorption behavior changed the color of the resultant solution from yellowish to pinkish, allowing naked-eye detection of Al^{3+} (see insert in Figure 3a).

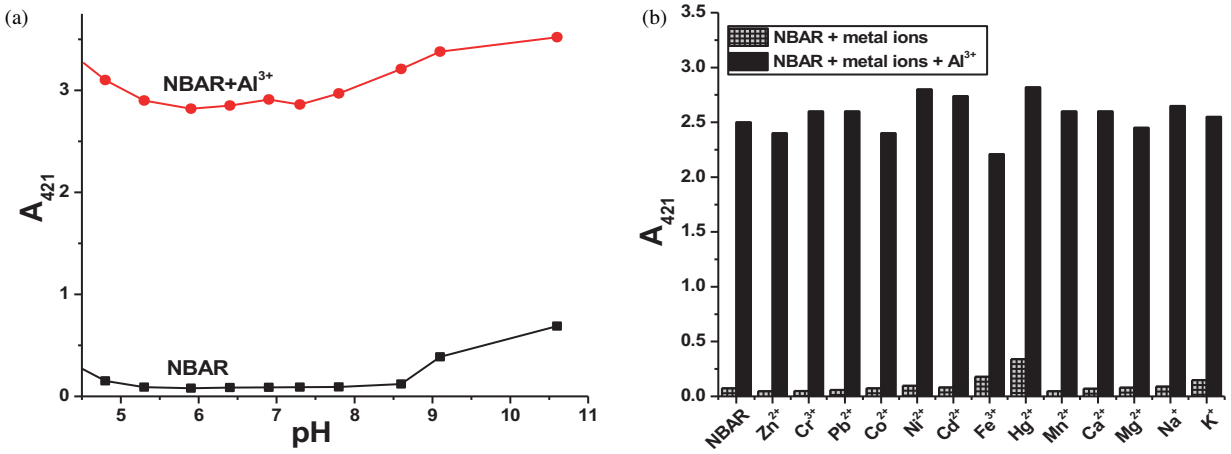

Figure 2. (a) Variation in absorption (421 nm) of NBAR and NBAR + Al^{3+} (20 μM each) at various pH values in ACN/H_2O (1/1, v/v) solution. (b) Absorption responses of 20 μM NBAR to the presence of various metal ions (gray bar) and the subsequent addition of Al^{3+} (black bar) in ACN/H_2O (v/v, 1:1, pH 6.80); the bars represent the absorption intensity at 421 nm.

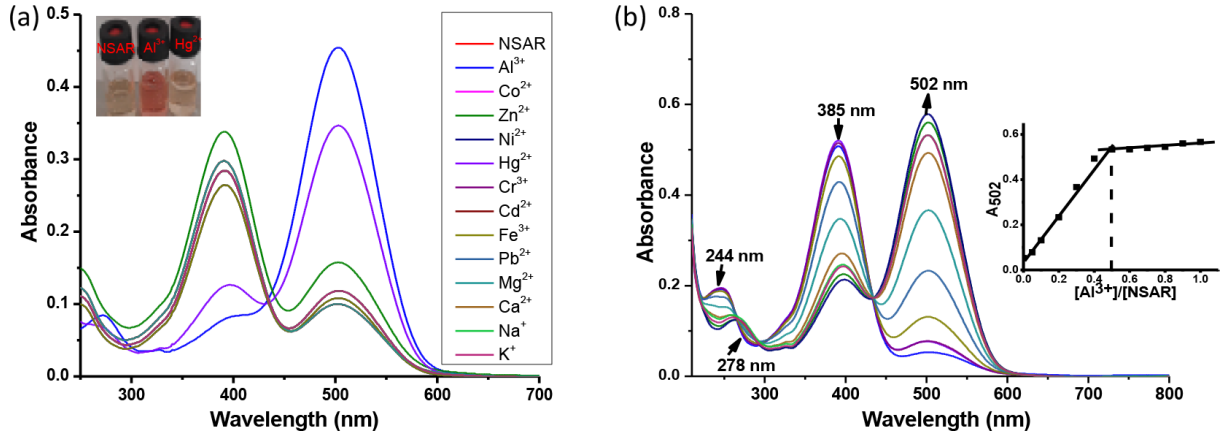

Figure 3. (a) Absorption responses of 20 μM NSAR to various metal ions (20 μM for Zn^{2+}, Cr^{3+}, Ni^{2+}, Hg^{2+}, Fe^{3+}, Al^{3+}, Pb^{2+}, Cd^{2+}, and Co^{2+}; 100 μM for Na^{+}, K^{+}, Mg^{2+}, and Ca^{2+}) in ACN/H_2O (1:1 v/v). (b) UV-vis spectra of NSAR (20 μM) with the addition of various concentrations of $AlCl_3$ (0, 1.0, 2.0, 4.0, 6.0, 8.0, 10.0, 12.0, 15.0, 18.0, and 20.0 μM, consecutively) in ACN/H_2O (1:1 v/v).

The effect of pH on NSAR and NSAR-Al^{3+} was monitored by absorption spectra. As seen in Figure 4a, the NSAR sensor had no response to hydrogen ions at pH between 5 and 8. These results demonstrate that Al^{3+} recognition by the NSAR sensor was barely interfered with by pH in the range from 5 to 8. We also examined the interferences from the other metal ions with NSAR in its response to Al^{3+}. The absorbance of NSAR with Al^{3+} was not affected significantly in the presence of any of the other metal ions tested, demonstrating little interferences from other metal ions (except Hg^{2+}, NSAR also gave a response to Hg^{2+} ions) (Figure 4b).

2.3. Binding studies

In this section, the binding properties of the complexes NBAR-Al^{3+} and NSAR-Al^{3+} were investigated. To investigate the binding mode of NBAR and Al^{3+}, Job's plot and absorption titration were carried out. Typical

UV-vis titration spectra for NBAR with Al^{3+} in ACN/water (v/v 1:1) are shown in Figure 1b (see insert). The absorbance titration curve showed a typical sigmoidal curve, inflecting at 0.5 equiv. of Al^{3+} and saturation of the absorbance was at ~0.5 equiv. of Al^{3+}. The titration experiments indicated that a 2:1 complex was formed between NBAR and Al^{3+}. The binding constant of this complex was calculated using absorption values at 421 nm by the equations described in the experimental section, and was determined to be 4.09×10^{11} M^{-2}.

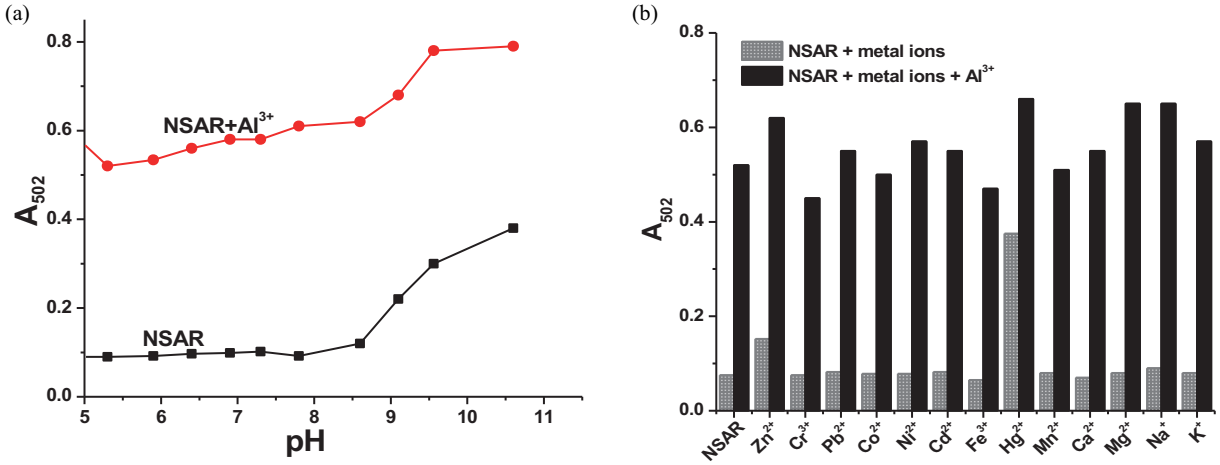

Figure 4. (a) Variation in absorption (502 nm) of NSAR and NSAR + Al^{3+} (20 μM each) at various pH values in ACN/H_2O (1/1, v/v) solution. (b) Absorption responses of 20 μM NSAR to the presence of various metal ions (gray bar) and the subsequent addition of Al^{3+} (black bar) in ACN/H_2O (1:1 v/v); the bars represent the absorption intensity at 502 nm.

Job's method was also applied to study the binding stoichiometry of NBAR and Al^{3+}. The Job's plot (Figure 5a) using a total concentration of 20 μM NBAR and Al^{3+} in ACN/water (v/v 1:1) solution exhibited a maximum absorbance (at 421 nm) when the molecular fraction of Al^{3+} and NBAR was close to 2:1, suggesting a 2:1 stoichiometry for the binding of NBAR and Al^{3+}.

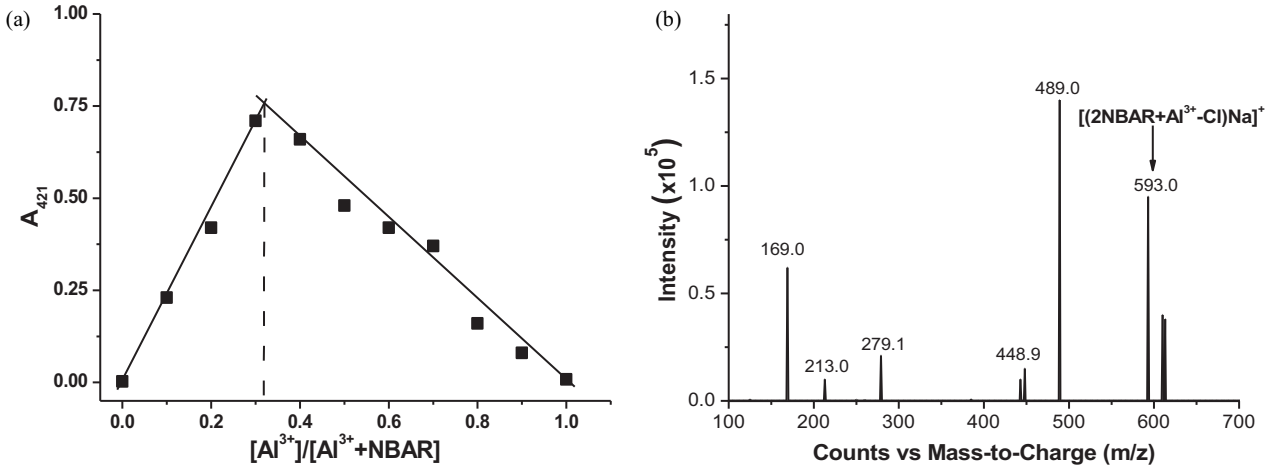

Figure 5. (a) Job's plot. The total concentrations of NBAR and Al^{3+} were kept constant at 20 μM and the absorption intensity was measured at 421 nm in the ACN/H_2O mixture. (b) ESI-mass spectrum of NBAR + Al^{3+}.

The species formed between NBAR and Al^{3+} were more accurately determined by ESI-MS. ESI-MS of the Al/NBAR solution (Figure 5b) shows an intense peak at m/z= 593, which is assignable to a 2:1 complex $[(2NBAR\text{-}Al\text{-}Cl)+Na]^+$ (m/z calcd = 593.0). This implies that Al^{3+} is in 5-coordination with the sensor with one chloride ion under the ESI-MS conditions.

For a good sensor, recognition reversibility is a significant requirement. We tested the reversibility of the binding between NBAR and Al^{3+} in ACN/water (v/v 1:1, pH 6.80) in the presence of Al^{3+} and EDTA (2.0 equiv.). The addition of EDTA (2.0 equiv.) to the solution of NBAR containing Al^{3+} caused the disappearance of the absorption signals of NBAR-Al^{3+} (Figure 6), suggesting that the chelation process is reversible. The possible structures of this process are shown in Scheme 2.

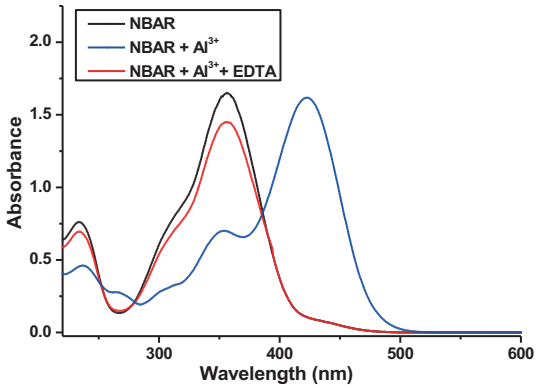

Figure 6. Reversibility of NBAR (20 μM) to Al^{3+} ions by EDTA. Black line: free NBAR (20 μM), blue line: NBAR + 0.5 equiv. of Al^{3+}, red line: NBAR + 0.5 equiv. of Al^{3+} + 1.0 equiv. of EDTA.

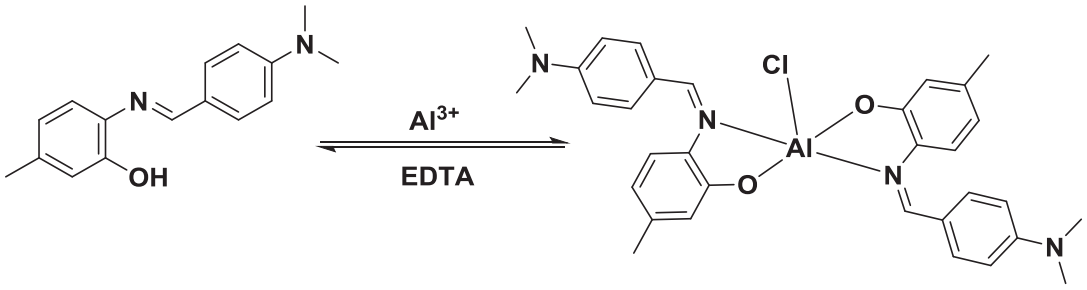

Scheme 2. The proposed reversible 2:1 binding mode between NBAR and Al^{3+}.

The corresponding quantitative analytical data (linear concentration range, RSD, limit of detection (LOD), limit of quantification (LOQ)) of NBAR were obtained and calculated. The absorbance is linearly dependent on the concentration of Al^{3+} in the range from 4.0 $\times$ 10^{-6} M to 4.0 $\times$ 10^{-5} M (R^2 = 0.967). Furthermore, the average absorbance values for the blank system (without Al^{3+}) were 0.095 (n = 8, RSD = 4.32%). LOD (3σ/slope) and LOQ (10σ/slope) were 3.6 $\times$ 10^{-6} M and 1.6 $\times$ 10^{-5} M, respectively.

Absorption titration and Job's plot methods were also applied to study the binding stoichiometry of NSAR and Al^{3+}. The absorbance titration curve (see insert in Figure. 3b) showed a typical sigmoidal curve, inflecting at 0.5 equiv. of Al^{3+}, and the saturation of the absorbance was at $\sim$0.5 equiv. of Al^{3+}. The titration experiments indicated that a 2:1 complex was formed between NSAR and Al^{3+}. The binding constant

of this complex was calculated using absorption values at 421 nm by the equations described in the experimental section, and was determined to be 1.65 $\times$ 10^{12} M^{-2}. The Job's plot (Figure 7) using a total concentration of 20 μM NSAR and Al^{3+} in ACN/water (v/v, 1:1) solution exhibited a maximum absorbance (at 502 nm) when the molecular fraction of Al^{3+} and NSAR was close to 2:1, suggesting a 2:1 stoichiometry for the binding of NSAR and Al^{3+}.

The reversibility of the recognition of NSAR was determined by adding EDTA to the complex NSAR-Al^{3+}. Due to the strong affinity of EDTA for Al^{3+} ions, an Al^{3+}-EDTA complex was formed, resulting in a disassociation of the NSAR-Al^{3+} and consequently an absorption decrease at 502 nm (Figure 8). Thus the complexation between NSAR and Al^{3+} is reversible. The possible structures of this process are shown in Scheme 3.

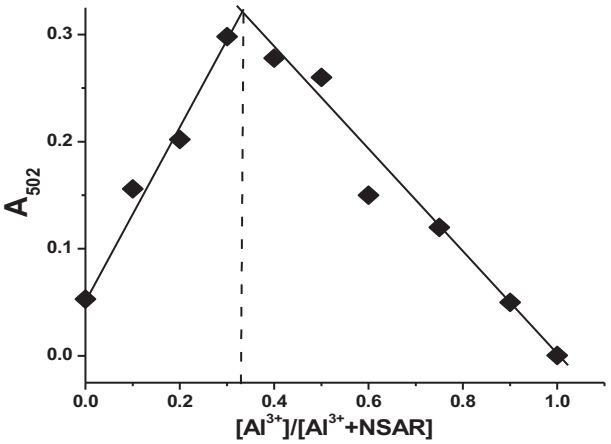

Figure 7. Job's plot. The total concentrations of NSAR and Al^{3+} were kept constant at 20 μM and the absorption intensity was measured at 502 nm in the ACN/H_2O mixture.

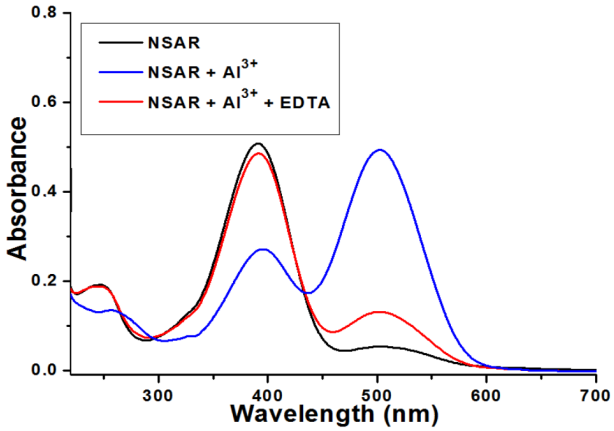

Figure 8. Reversibility of NSAR (20 μM) to Al^{3+} ions by EDTA. Black line: free NSAR (20 μM), blue line: NSAR + 0.5 equiv. of Al^{3+}, red line: NSAR + 0.5 equiv. of Al^{3+} + 1.0 equiv. of EDTA.

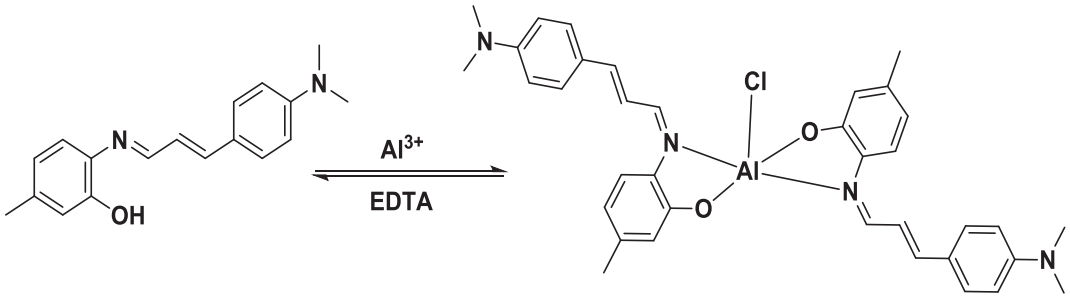

Scheme 3. The proposed reversible 2:1 binding mode between NSAR and Al^{3+}.

The linear concentration range, RSD, LOD, and LOQ of NSAR were also studied. The absorbance was linearly dependent on the concentration of Al^{3+} in the range from 4.0 $\times$ 10^{-6} M to 1.0 $\times$ 10^{-4} M (R^2 = 0.991). Furthermore, the average absorbance values for the blank system (without Al^{3+}) were 0.110 (n = 8, RSD = 3.05%). LOD and LOQ were estimated to be 4.21 $\times$ 10^{-6} M and 1.86 $\times$ 10^{-5} M, respectively.

In summary, we developed two Schiff base derivatives, NBAR and NSAR, for selective detection of Al^{3+} in aqueous solution. NBAR and NSAR receptors harbored a 1N1O Al^{3+}-receptor moiety and bound Al^{3+} in

a 2:1 stoichiometry with apparent binding constants 4.09 $\times$ 10^{11} M^{-2} and 1.65 $\times$ 10^{12} M^{-2}, respectively. The receptors displayed a distinct change in color and absorption upon the alteration of free Al^{3+} levels in solution with a reversible response and little interference with other biologically relevant metal ions (except Hg^{2+}, NSAR also gave a response to Hg^{2+}).

3. Experimental

3.1. Materials and instrumentation

2-Amino-5-methyl phenol, 4-(dimethylamino)benzaldehyde, and 4-(dimethylamino) cinnamaldehyde were purchased from Sigma-Aldrich Chemie GmbH (Steinheim, Germany). Other chemicals and solvents used in the experiments were purchased commercially. The solutions of metal ions were prepared from chloride salts of Ni^{2+}, Fe^{3+}, Mn^{2+}, Hg^{2+}, Na^{+}, Ca^{2+}, Zn^{2+}, and Al^{3+}; and nitrate salts of Mg^{2+}, Pb^{2+}, K^{+}, and Co^{2+}. Stock solutions of metal ions (10 mM) were prepared in deionized water, except for Fe^{3+}, which was dissolved in 0.1 M HCl. A stock solution of the receptors (NBAR and NSAR (10 mM)) was prepared in ACN. The solution of the receptors was diluted to 20 μM with ACN/H_2O (1:1 v/v). In the selectivity experiments, the test samples were prepared by appropriate amounts of metal ion stocks into 1 mL of solution of the receptors (20 μM).

All ^{1}H NMR (400.1 MHz) and ^{13}C NMR spectra were recorded at 25 °C with deuterated DMSO and $CDCl_3$ in a Bruker NMR spectrometer (Bruker Ultrashield Plus Biospin Avance III 400 MHz NaNoBay FT-NMR). ESI-MS analyses were performed using an LC-MS/MS mass spectrometer (Agilent LC-MS/MS 6460 Triple Quadrupole). UV/vis spectra were recorded on a Shimadzu UV-1800 spectrophotometer at 293 K. The pH measurements were carried out on a Corning pH meter equipped with a Sigma-Aldrich micro combination electrode calibrated with standard buffer solutions.

3.2. Synthesis and characterization of the receptors

3.2.1. Preparation of (2-(4-(dimethylamino)benzylideneamino)-5-methylphenol (NBAR)

4-(Dimethyl)aminobenzaldehyde (500 mg, 3.35 mmol) and 2-amino-5-methylphenol (410 mg, 35 mmol) were mixed and stirred for 2 h in ethanol (10 mL) at room temperature. The reaction was monitored by TLC [hexane:ethylacetate (3/1)]. A yellow precipitate product was washed with cold ethanol and dried under vacuum. Yield 0.73 g (86%). ^{1}H NMR (400 MHz, $CDCl_3$)δ: 8.24 (s, 1H), 7.79 (d, J = 8.9 Hz, 2H), 7.28 (s, 1H), 6.86 (d, J = 8.3 Hz, 1H), 6.76 (d, J = 8.9 Hz, 2H), 6.68 (d, J = 9.2 Hz, 1H), 6.64 (s, 1H), 3.06 (s, 6H), 2.33 (s, 3H). ^{13}C NMR (100 MHz, $CDCl_3$)δ: 158.28, 153.04, 152.30, 145.24, 133.75, 130.10, 124.96, 118.66, 117.01, 113.06, 111.65, 40.22, 18.00. ESI-MS (positive mode) m/z 255.2 $[M+H]^+$.

3.2.2. Preparation of 3-(4-(dimethylamino)phenyl)allylidene)amino)-5-methylphenol (NSAR)

4-(Dimethyl)aminocinnamaldehyde (500 mg, 2.85 mmol) and 2-amino-5-methylphenol (350 mg, 2.85 mmol) were mixed and stirred for 4 h in ethanol (10 mL) at room temperature. The reaction was monitored by TLC [hexane:ethylacetate (3/1)]. A red precipitate product was washed with cold ethanol and dried under vacuum. Yield 0.64 g (80%). ^{1}H NMR (400 MHz, $CDCl_3$)δ 8.08 (d, J = 3.7 Hz, 1H), 7.42 (t, J = 19.0 Hz, 2H), 7.26 (s, 3H), 7.10–6.92 (m, 2H), 6.71 (dd, J = 34.8, 26.1 Hz, 3H), 3.35–2.73 (m, 6H), 2.30 (d, J = 23.7 Hz, 3H).

^{13}C NMR (100 MHz, $CDCl_3$)δ 152.86, 150.70, 147.17, 146.55, 135.82, 132.62, 129.67, 127.82, 124.24, 123.73, 119.21, 117.39, 112.89, 42.01, 21.4. ESI-MS (positive mode) m/z 281.2 $[M+H]^+$.

3.3. Binding studies

Al^{3+}-binding titration and Job's plots were obtained for the receptors to determine the stoichiometry between Al^{3+} and the receptors. For Job's plot, the total molar concentrations of the receptors and Al^{3+} were held constant, but their mole fractions were varied. Then, absorption spectra of these fractions were collected. In addition, absorption values at maximum were plotted against the mole fractions of the receptors and Al^{3+}. Typical UV-vis titration experiments for the receptors were performed by the following process. A solution of the sensor (10 mM, prepared in ACN) was first diluted to 20 μM with ACN/H_2O (v:v, 1:1) and the absorption spectra were recorded in a quartz cell. Then Al^{3+} solution (10 mM, prepared in water) was introduced in portions of 2, 4, 6, 10, 12, 14, 16, 18, and 20 μM, consecutively (20 μL corresponds to 1 equiv.) to each of the sensor's solutions (20 μM, 1 mL). The spectra were recorded 5 min after each addition. The binding constants were estimated by using the absorption titration results. The equation below was used to calculate the binding constants for 2:1 complexes.[32]

$$S + 2L \rightleftharpoons SL_2 \tag{1}$$

The apparent binding constant and the fraction of the ligand that participates in the complex are shown in Eqs. (2) and (3).

$$K = \frac{[AlS_2]_e}{[Al]_e\ [S]_e^2} \tag{2}$$

The subscript e means concentrations at equilibrium. The ratio of the equilibrium between the complex, $[SAl]_e$, and the initial concentration of the receptors, $[S]_o$, can be derived from the absorbance of the receptors at a chosen wavelength when the system is at equilibrium. The result of the derivation is shown in Eq. (4).

$$Fc = \frac{Au - Am}{2Au - 2Ac} \tag{3}$$

F_c is the fraction of Al^{3+} that formed a complex, $[SAl]_e$ is concentration at equilibrium, and $[Al]_0$ is the initial concentration. A_u, A_m, and A_c are the absorbances of solutions of Al^{3+} (before any Al^{3+} was added), during the titration and at saturation, respectively.

Finally, the integrated apparent binding constant equation is shown in Eq. (4) (for a complete derivation see ref. 32).

$$K = \frac{Fc}{2\,[S]_o[Al]_e\,(1 - Fc)^2} \tag{4}$$

Acknowledgment

The authors are grateful to Osmaniye Korkut Ata University for financial support (Project Number: OKUBAP-2015-PT2-010).

References

1. Bertini, I.; Gray, H. B.; Stiefel, E. I.; Valentine, J. S. *Biological Inorganic Chemistry*; University Science Books, Sausalito, CA, USA, 2006.
2. Niquette, P.; Monette, F.; Azzouz, A.; Hausler, R. *Water Qual. Res. J. Canada* **2004**, *39*, 303-310.
3. Exley, C. *J. Inorg. Biochem.* **2005**, *99*, 1747-1748.
4. Saiyed, S. M.; Yokel, R. A. *Food. Addit. Contam.* **2005**, *22*, 234-244.
5. Gramiccioni, L.; Ingrao, G.; Milana, M. R.; Santaroni, P.; Tomassi, G. *Food. Addit. Contam.* **1996**, *13*, 767-774.
6. Alvim, M. N.; Ramos, F. T.; Oliveira, D. C.; Isaias, R. M. S.; Franca, M. G. C. *J. Biosci.* **2012**, *37*, 1079-1088.
7. Barceló, J.; Poschenrieder, C. *Environ. Exp. Bot.* **2012**, *48*, 75-92.
8. Braydich-Stolle, L. K.; Speshock, J. L.; Castle, A.; Smith, M.; Murdock, R. C.; Hussain, S. M. *ACS Nano.* **2010**, *4*, 3661-3670.
9. Klein, G. L. *Curr. Opin. Pharmacol.* **2005**, *5*, 637-640.
10. Berthon, G. *Coord. Chem. Rev.* **2002**, *228*, 319-341.
11. Flaten, T. P. *Brain Res. Bull.* **2001**, *55*, 187-196.
12. Good, P. F.; Olanow, C. W.; Perl, D. P. *Brain Res.* **1992**, *593*, 343-346.
13. Walton, J. R. *Encycl. Environ. Health* **2011**, 331-342.
14. 14. Krejpcio, Z.; Wojciak, R. W. *Pol. J. Environ. Stud.* **2002**, *11*, 251-254.
15. 15. Barcelo, J.; Poschenrieder, C. *Environ. Exp. Bot.* **2002**, 4875-4892.
16. Nomizu, T.; Kaneco, S.; Tanaka, T.; Ito, D.; Kawaguchi, H.; Vallee, B. T. *Anal. Chem.* **1994**, *66*, 3000-3004.
17. Sanz-Medel, A.; Cabezuelo, A. B. S.; Milacic, R.; Polak, T. B. *Coord. Chem. Rev.* **2002**, *228*, 373-383.
18. Norouzi, P.; Gupta, V. K.; Larijani, B.; Rasoolipour, S.; Faridbod, F.; Ganjali M. R. *Talanta* **2015**, *131*, 577-584.
19. Chien, J. C. W.; Westhead, E. W. *Biochemistry* **1971**, *10*, 3198-3203.
20. 20. Lian, H.; Kang, Y.; Bi, S.; Arkin, Y.; Shao, D.; Li, D.; Chen, Y.; Dai, L.; Gan, N.; Tian, L. *Talanta* **2004**, *62*, 43-50.
21. Chemate, S.; Sekar, N. *Sens. Actuators B* **2015**, *220*, 1196-1204.
22. Lia, C.; Zhoua, Y.; Li, Y., Zoua, C., Konga, X. *Sens. Actuators B* **2013**, *186*, 360-366.
23. Sen, B.; Mukherjee, M.; Banerjee, S.; Pal, S.; Chattopadhyay, P. *Dalton Trans.* **2015**, *44*, 8708-8717.
24. Sahana, A.; Banerjee, A.; Lohar, S.; Sarkar, B.; Mukhopadhyay, S. K.; Das, D. *Inorg. Chem.* **2013**, *52*, 3627-3633.
25. 25. Qin, J. C.; Yang, Z. Y. *Synt. Met.* **2015**, *209*, 570-576.
26. Qin, J. C.; Yang, Z. Y.; Li, T. R.; Wang, B. D.; Fan, L. *Synt. Met.* **2014**, *195*, 141-146.
27. Sarkar, D.; Pramanik, A.; Biswas, S.; Karmakar, P.; Mondal, T. K. *RSC Adv.* **2014**, *4*, 30666-30672.
28. Zhang, Y. G.; Shi, Z. H.; Yang, L. Z.; Tang, X. L.; An, Y. Q.; Ju, Z. H.; Liu, W. S. *Inorg. Chem. Commun.* **2014**, *39*, 86-89.
29. Chen, W.; Jia, Y., Feng, Y.; Zheng, W.; Wang, Z.; Jiang, X. *RSC Advances* **2015**, *5*, 62260-62264.
30. Xue, D.; Wang, H.; Zhang, Y. *Talanta* **2014**, *119*, 306-311.
31. Peralta-Domínguez, D.; Rodríguez, M.; Ramos-Ortíz, G.; Luis Maldonadoa, J.; Meneses-Navaa, M. A.; Barbosa-Garcíaa, O.; Santillan, R.; Farfánc, N. *Sens. Actuators B* **2015**, *207*, 511-517.
32. Perez, C. A.; Wei, Y.; Guo, M. *J. Inorg. Biochem.* **2009**, *103*, 326-322.